

Binary fluid demixing: The crossover region

Ignacio Pagonabarraga

Departament de Física Fonamental, Universitat de Barcelona,
Av. Diagonal 647, 08028-Barcelona, Spain

Alexander J. Wagner and M.E. Cates

Department of Physics and Astronomy, University of Edinburgh,
JCMB Kings Buildings, Mayfield Road, Edinburgh EH9 3JZ, U.K.

By performing lattice Boltzmann simulations of a binary mixture, we scrutinize the dynamical scaling hypothesis for the spinodal decomposition of binary mixtures for the crossover region, *i.e.* the region of parameters in the growth curve where neither inertia nor viscous forces dominate the coarsening process. Our results give no evidence for a breakdown of scaling in this region, as might arise if the process were limited by molecular scale physics at the point of fluid pinch-off between domains. A careful data analysis allows us to refine previous estimates on the width of the crossover region which is somewhat narrower than previously reported.

I. INTRODUCTION

Spinodal decomposition occurs when a binary mixture, which forms a homogeneous phase at high temperature, undergoes spontaneous demixing after imposing a sudden quench to below the spinodal temperature of the mixture. Following the quench, after a short period of interdiffusion, the mixture will form domains of different composition, separated by sharply defined interfaces. In its late stage, the local compositions of the fluid domains correspond to those of the two bulk phases at coexistence, while the interfacial tension approaches its equilibrium value. The shape and evolution of the domains will depend on the initial composition of the mixture, as well as on the different physical parameters characterizing the fluids. For the case of a symmetric mixture, in which the amounts and properties of the two immiscible species are the same, then starting from a randomly mixed initial state, bicontinuous structures develop.

As emphasized by Siggia[1] and Furukawa[2], the physics of spinodal decomposition involves capillary forces, viscous forces and fluid inertia. Local interfacial curvature generates stress which drives fluid motion; this will propagate by viscous force or inertial motion (or both) depending on the parameters of the fluid. If we assume no other physics determines the spinodal process, the parameters determining the fluid behavior are then the interfacial tension, σ , fluid mass density, ρ , and viscosity η (for a deep quench, diffusion does not contribute significantly beyond a short initial transient). Any degree of asymmetry in the mixture's composition or in the dynamical properties of the fluids will provide additional control parameters.

For the completely symmetric case, from the three relevant fluid parameters only one length, L_0 , and one time, T_0 , can be constructed: $L_0 = \eta^2/(\rho\sigma)$ and $T_0 = \eta^3/(\rho\sigma^3)$. The absence of other physical mechanisms controlling the spinodal decomposition in the late-stage domain growth leads to the *dynamical scaling* hypothesis[1, 2]. According to it, if we express the domain size, $L(T)$ as a function of time T in reduced units using the characteristic length and time scales, the corresponding dimensionless length $l \equiv L/L_0$, expressed in terms of the dimensionless time $t \equiv T/T_0$, will be a universal scaling function

$$l = l(t) \tag{1}$$

the same for all fully symmetric, binary incompressible fluid mixtures. The use of scaling concepts has been of extreme help in understanding and rationalizing the physics underlying complex phenomena. In the present problem, the dynamical scaling states that all fluids will have a unique domain growth rate governed only by the value of L/L_0 , which controls the dominance of viscous or inertial fluid transport. Therefore, this scaling expression provides a systematic and simple way to analyze the spinodal decomposition of any fluid, in terms of its basic physical mechanisms.

Furukawa (following Siggia) [1, 2] analyzed the limiting behavior of the proposed universal function $l(t)$. For small enough t fluid inertia is negligible compared to viscous forces, while for large t the opposite is true[3]. Balancing the dominant terms in the Navier-Stokes equation in each case leads to the asymptotes

$$l(t) \rightarrow \begin{cases} bt & ; \quad t \ll t^* \\ ct^{2/3} & ; \quad t \gg t^* \end{cases} \tag{2}$$

where t^* stands for the crossover time, when the viscous and inertial contributions are comparable. This can be defined more precisely as the time at which the extrapolated viscous and inertial asymptotes of the $l(t)$ cross each

other on a log-log plot. For intermediate times around t^* , the universal function $l(t)$ will exhibit a smooth crossover from the viscous to the inertial asymptotic behavior. It is important to remark that dynamical scaling implies the universality, not just of the asymptotic power laws for the scaling function $l(t)$, but of the entire curve, and accordingly of the amplitudes b , c and t^* .

Although there is good experimental evidence for the viscous growth regime[5], the inertial regime is more difficult to study experimentally[4, 6]. Therefore, simulation techniques have so far been the basic tools to analyse the different growth regimes and validate the scaling hypothesis [6, 7, 8, 9]. (The ease with which fully symmetric immiscible fluids can be created on a computer, compared to the laboratory, is also a factor.) Such scaling has allowed classification and comparison of (previously scattered) simulation results as well as a critical analysis of the derived parameters (such as b), revealing a number of discrepancies in the published data (mainly related to residual diffusion and/or finite size effects)[6]. In our view, the existence of a viscous scaling regime (with a universal b) is now fairly clearly established in three dimensions. (The case of two dimensions is quite different [16, 17].) The search for an asymptotic inertial regime has likewise been extended carefully up to Reynolds numbers of order 300 (with Reynolds number defined as $Re = L\dot{L}\rho/\eta = \dot{l}l$). Although there is still a controversy regarding the true final asymptote at sufficiently high Reynolds number[4, 10], previous work[6, 7] does establish the existence of a well defined asymptotic inertial regime, at least as far as the $l(t)$ curve is concerned, at relatively modest $Re \geq 100$. The attainment of asymptotic behaviour in this region of $l(t)$ (roughly, $3 \times 10^3 < l < 3 \times 10^5$) is less obvious when one examines velocity statistics[6] or interfacial dynamics[11]. However, further exploration at still higher Re (say, $l \geq 10^6$) remains out of reach with present simulation methods.

Compared to the status of the viscous and inertial regimes, the existence of dynamical scaling in the crossover regime remains to be established. So far it was reported in [6, 7] that the crossover region spans four decades in dimensionless time, and that the crossover time t^* , although formally of order one, is about 10^4 . But the lattice Boltzmann data presented in [6] is in fact relatively sparse for the crossover region, and does not allow a direct check of the proposed collapse onto a universal curve.

There are, however, some results found using dissipative particle dynamics [9] which lie within the crossover regime as determined in [6]. Jury et al [9] reported incomplete collapse of this data: each dataset had a similar slope but the curves did not join up on the $l(t)$ plot. Their data was found to be broadly compatible with logarithmic deviations from dynamic scaling. Although the more recent (lattice Boltzmann) results obtained in [7] suggest that those deviations may instead be due to finite size effects, the validity of dynamical scaling within the crossover region is far from completely established.

Jury *et al.* noted that the dynamical scaling hypothesis relies on the assumption that viscous forces and inertia are the *only* physical mechanisms controlling domain growth. Other physics is, however, involved too: we have already mentioned diffusion, which can however be kept negligible, on the domain scale, for deep quenches (see Ref.[6] for a discussion of this). Another mechanism that must be present during the domain growth arises during topological reconnection or *pinch-off* events. These events are necessary for the coarsening of the bicontinuous structure. They correspond to the contraction of a fluid neck to zero width in a finite time (see e.g. Ref.[11] for visualizations of the evolution and rupture of necks in the different regimes of spinodal decomposition). Unless diffusion intervenes first, the final stage of such a reconnection event always involves a microscopic, molecular, length scale. Moreover, recent studies indicate that such reconnection events follow a distinct scaling of the dynamics[12, 13] that might, in principle, interfere somehow with the scaling law for the domain size. It is not clear whether this could happen only in the crossover region and not in the viscous or inertial asymptotes, but nonetheless, there is enough uncertainty to warrant a detailed study of the crossover domain, which we now present.

II. MODEL

Spinodal decomposition with a deep quench is essentially a problem of deterministic, isothermal fluid motion coupled to moving interfaces, in which it is important to deal with pinch-off events consistently. As already mentioned, diffusion is irrelevant, and thermal fluctuations can also be disregarded at long times. To study this process we have therefore used the lattice Boltzmann method. This is a simulation technique in which the interfaces emerge as a result of the imposed free energy. This fact has some advantages with respect to other standard numerical techniques to study Navier-Stokes equations. The details of the model for the case of a binary mixture we have used are described elsewhere[6, 14, 15]. The model simulates a binary mixture with the model free energy

$$F = \int d\mathbf{r} \left\{ -\frac{A}{2}\phi^2 + \frac{B}{4}\phi^4 + \frac{1}{3}\rho \log \rho + \frac{\kappa}{2}|\nabla\phi|^2 \right\}, \quad (3)$$

in which A , B are parameters that control the phase behavior of the mixture. When $A < 0$ and $B > 0$ two phases coexist in equilibrium. In Eq.3, ϕ is the usual order parameter (the normalized difference in number density of the

two fluid species), and if $A = B$, the order parameter in the coexisting low temperature phases takes values $\phi = \pm 1$. (This is a matter of convention, not of physics.) The parameter κ is related to the energy cost of generating a spatial gradient. It determines the value of the interfacial width, $\xi = 5\sqrt{\kappa/2A}$, and the surface tension $\sigma = \sqrt{8\kappa A^3/9B^2}$. Finally, ρ is the total fluid density, which remains essentially constant during phase separation. (This is ensured by working at very low Mach numbers.)

The lattice Boltzmann model for a binary mixture involves two velocity distribution functions, f and g , on a discrete lattice with a discrete time relaxational dynamics. The properties of the model are fixed through the equilibrium distributions towards which f and g relax; the zeroth, first and second moments of f determine the density, the momentum flux, and the stress tensor, while moments of g determine ϕ and the order parameter flux. In this way the dynamics of the distribution functions is connected to the macroscopic behavior of the fluid. It has been shown that the Navier-Stokes and advective-diffusion equations are recovered as the hydrodynamic limit of the corresponding lattice Boltzmann dynamics[15], at least in the incompressible limit[6]. The form of the pressure tensor depends on the free energy model chosen[15].

The spontaneous emergence of interfaces as a result of the imposed free energy, eq.(3), is an appealing feature of this method. However, as a result the interfaces are not structureless, but have finite width ξ . In practice, the parameters of the free energy are chosen such that ξ remains around 3 lattice spacings in all runs; this minimizes anisotropy effects due to the underlying lattice. The finite width imposes restrictions on the length scales that can accurately be studied with this method. In real fluids (deeply quenched) the interfacial width is a few atomic diameters, whereas we are often in the regime of $\xi \gg L_0$ (especially for the most inertial runs), which is much larger. For spinodal decomposition this should not matter as long as the dynamical scaling hypothesis holds. However, if the interfacial width turns out to be dynamically relevant, as could possibly apply during pinch-off, the variation between runs of ξ/L_0 has to be taken into account.

Since we are interested in testing the dynamical scaling hypothesis in the absence of diffusion, the mobility must also be chosen to ensure that, after a short initial transient which is always dominated by diffusion (when the initial domains are formed) diffusion gives an irrelevant contribution to the growth rate. This can be done using protocols described in[6].

III. METHOD AND RESULTS

We have performed a number of new lattice Boltzmann simulations on large (256^3) lattices, with parameters chosen to explore the crossover region, as well as a couple of runs deeper into the viscous and inertial regimes to clarify the convergence to the corresponding asymptotic regimes. These add significantly more data to those presented previously in [6, 7], where the focus was on the asymptotes rather than the crossover regime. We start with random initial conditions (effectively infinite temperature), and choose the parameters in the free energy, eq.(3), such that $B > 0$ and $A = -B$. This is equivalent to performing a sudden deep quench below the spinodal temperature of the mixture (which corresponds to $A = 0$). We then follow the subsequent evolution of the system by computing the characteristic domain size $L(T)$, which is then converted to reduced physical units.

There are several different ways to measure the domain size in a binary mixture[6]. Here we choose to employ a characteristic length scale extracted from the curvature of the interface (see Ref.[16]). The latter is a tensor, defined by

$$D_{\alpha\beta} = \frac{\sum_{lattice} \partial_\alpha \phi \partial_\beta \phi}{\sum_{lattice} \phi^2} \quad (4)$$

where α and β refer to the three spatial coordinates, and ∂_α means the spatial derivative with respect to the α component of the spatial coordinate. The three eigenvalues of this matrix λ_i are then three characteristic inverse lengths. From them, the domain size, L , can be estimated as

$$L = \frac{3}{\lambda_1 + \lambda_2 + \lambda_3} \quad (5)$$

Strictly speaking, this is a square of a length; it is related to the product of two characteristic lengths. However, the second relevant length for the order parameter gradients in the system is the interfacial width. This is the same for all the simulations; hence, it contributes a constant factor of order unity to eq.(5). We have monitored the values of the domain size as a function of time after the quench, $L(T)$. Before seeking data collapse by converting to reduced physical units, it is very important to select the subset of reliable data from each simulation run. Early in each run one always has a period of interdiffusion, followed by a regime where diffusion and hydrodynamics are both present. Only when the diffusive contribution to the coarsening rate becomes small can the $L(T)$ data be expected to scale

onto the universal $l(t)$ curve. (We removed the early time data by eye but the cutoff values we used were comparable to those that V. Kendon obtained by a more rigorous procedure [6].) On the other hand, it is found that when the domain size is much larger than about a quarter of the simulation box, finite size effects start to be relevant. Hence, from each simulation only a central portion of the overall data can be relied upon; this data covers at most one decade or so in time [6]. As a result, the full crossover region cannot be spanned by a single run but only by varying simulation parameters to access $l(t)$ one section at a time. Since other parameters, such as ξ/L_0 , are varying during this procedure, there is no guarantee, in general, of a smooth joining up of the curves. In table I we show the set of fluid parameters we have used to explore the crossover regime. We have also added a couple of sets that lie in the asymptotic regimes to check that the universal viscous and inertial scaling regimes are indeed recovered.

The initial period of diffusive growth, in each run, means that the reduced physical time must be defined as $t = (T - T_{int})/T_0$, where the offset time T_{int} is not known a priori, and can vary from one run to another. Previously, Kendon *et al.* developed a careful procedure for fitting this parameter [6], separately for each run, using the data from that run only. Although this is an objective procedure, the fitted values of T_{int} are very sensitive to the details of the fitting, and the precise location of the resulting $l(t)$ data is similarly sensitive. In the current work, therefore, we leave T_{int} as a free parameter for each run, and then globally optimize the choices of all the T_{int} 's to achieve the best data collapse on the $l(t)$ curve. This is best done by human eye using an interactive graphics routine. The T_{int} values are displayed in table II; given the uncertainties, these are broadly consistent with the ones obtained previously.

We show in Fig.1 the scaling curve we have obtained in this fashion for all the runs of table I. One can clearly see that all the simulation data can thereby be made to fall on a universal scaling curve, with overlapping datasets extending from the viscous regime deep into the inertial one. We have also drawn the two lines that correspond to the viscous and inertial asymptotic laws to display how these are attained at either end of the crossover. Since we are using a definition for the domain size different from that of Ref.[6], we have to recompute the amplitudes of the asymptotic law. These are $b = 0.065$ and $c = 1.3$, which gives a crossover time $t^* = 10^4$. Our crossover region now spans about two decades, somewhat narrower than the previous estimates; in particular, runs that were previously taken to lie in the late crossover [6, 11, Run29, Run30] are found to be much closer to the asymptote than previously suggested. The reduced crossover width is more in line with normal expectations and suggests that uncertainty in the determination of T_{int} by the previous method [6, 7] led to an exaggeration of the crossover.

In Fig.2 we zoom in on the initial part of the crossover region. It is apparent how (to within small errors), the different runs lie on top of each other, as pieces of a continuous universal curve. It is interesting to look at Run13. Although in general, one run spans only one dynamical regime (due to the reasons explained at the beginning of the section), Run13 clearly exhibits a linear growth followed by a deviation, at the beginning of the crossover region. That this is not a finite-size artifact is clear, since runs that lie further in the crossover region coincide with the final portion of Run13.

In Fig.3 we have focused on the late part of the crossover region. Again, one can clearly see how different runs lie on top of each other. The relaxation towards the final, inertial growth law is faster than previously predicted. There is no evidence of any kind of deviations. This nice collapse into a single curve rules out the logarithmic deviations [9] that could be attributed to the emergence of a new length scale in this dynamical regime.

Our procedure for choosing T_{int} (by optimizing data collapse) is less objective than the one used previously by Kendon *et al.* [6] and it is not surprising that the resulting scaling is better. However, the sensitivity to T_{int} , and the quality of the collapse when this is allowed to float, leads us to conclude that there is no firm evidence *against* dynamical scaling in the crossover region, despite the previous results of Jury *et al.* [9].

Of course, since the fitting is done by human eye, there is a danger, perhaps, of seeing scaling where none exists. To check this, we have tried the same procedure in two dimension where scaling is indeed held not to exist (at least, not for bicontinuous morphologies) [16, 17]. The same approach to the data does not give similar collapse of the two dimensional data, which is reassuring.

As a further validation of our approach, we have also checked our results by computing the domain size using an independent domain size measurement. Specifically, for Runs 3, 4, 7, 13, 20 and 29 we have computed the spherically averaged order parameter structure factor

$$S(k, T) \equiv \int_{|\mathbf{k}|=k} \phi(\mathbf{k}, T) \phi(-\mathbf{k}, T) d^3\mathbf{k} \quad (6)$$

from it, we can obtain a measure of the mean domain size as the inverse of its first moment,

$$L_\phi(T) = \frac{\int S(k, T) dk}{\int k S(k, T) dk} \quad (7)$$

In this way we again sample the universal curve from the viscous up to the inertial regime. We have used the values of T_{int} obtained from L to construct the universal curve for L_ϕ . In fig. 4 we show the different runs after scaling

appropriately, which shows that we are able to collapse all the data on a single universal curve. It exhibits the two asymptotic viscous and inertial regimes. The fact that we are able to use the obtained values of T_{int} to construct the universal curve using independent measures of the domain lengths gives confidence that the scaling procedure we have followed is robust. If we compare the $l(t)$ curves obtained from the two domain lengths, we see that the ones derived from $L(T)$ tend to lie above those corresponding to L_ϕ . However, in fig.5 we compare the scaled curves obtained using the two length measures for a few runs. For run 29 we have estimated the error in the measure as the mean square deviation of three length-scales measured as $1/\lambda_1$, $1/\lambda_2$ and $1/\lambda_3$ (see eq. (5)), which we display as upper and lower bars. The error in the determination of the domain size, which is around 5%, does not allow to distinguish, in the late portion of the runs, between the two measures. This analysis also shows that the slight deviations from scaling visible in Fig. 2 are well within the error tolerances expected[18].

IV. CONCLUSIONS

In this paper we have analyzed in detail the crossover region of the spinodal decomposition of a binary mixture. By performing a number of new large lattice Boltzmann simulations, we have covered the regime where viscous forces and inertial transport are simultaneously relevant. Throughout the crossover, the data is compatible with the existence of a universal scaling curve $l(t)$ in reduced physical units. The crossover region is somewhat narrower than previously reported. This can be attributed to the uncertainties in the behavior in the late part of the crossover arising from the ambiguities in the determination of the fitting parameter T_{int} . The existence of the scaling curve argues against the suggestion [9] that the physics of pinch-off events can strongly interfere with the domain growth in this regime of parameters.

Acknowledgments

This work was funded in part by EPSRC Grant GR/M56234 and EC Access to Research Infrastructure Contract HPRI-1999-CT-00026 TRACS programme at EPCC. .

-
- [1] E. Siggia, Phys. Rev. A **20**, 595 (1979)
 - [2] H. Furukawa, Phys. Rev. A **31**, 1103 (1985)
 - [3] In the latter, since the interfacial area and the kinetic energy are both decreasing, the stated balance cannot be maintained in the energy equation unless an energy cascade is introduced, in which the reduction in interfacial area at large scales feeds kinetic energy down to smaller scales where viscous dissipation finally removes energy from the system. A three-length scales analysis predicts, nonetheless, the same primary balance that can be obtained directly from the Navier-Stokes equation (differences in the scaling of the velocity fields are obtained, though)[4].
 - [4] V.M. Kendon, Phys. Rev. E **61**, R6071 (2000)
 - [5] P. Guenoun, R. Gastaud, F. Perrot and D.Beysens, Phys. Rev. A **36**, 4876 (1987)
 - [6] V.M. Kendon, M.E. Cates, I. Pagonabarraga, J.-C. Desplat, and P. Bladon, J. Fluid Mech. , () in press cond-matt/0006026
 - [7] V.M. Kendon, J.-C. Desplat, P. Bladon, and M.E. Cates, Phys. Rev. Lett. **83**, 576 (1999)
 - [8] C. Appert, J.F. Olson, D.H. Rothman, and S. Zaleski, J. Stat. Phys. **81**, 181 (1995); S. Bastea, and J.L. Lebowitz, Phys. Rev. E **52**, 3821 (1995); M.Laradji, S. Toxvaerd, and O.G. Mouritsen, Phys. Rev. Lett. **77**, 2253 (1996)
 - [9] S.I. Jury, P. Bladon, S. Krishna, and M.E. Cates, Phys. Rev. E **59**, 2535 (1999)
 - [10] M. Grant and K.R. Elder Phys. Rev. Lett. **82**, 14 (1999)
 - [11] I. Pagonabarraga, J.-C. Desplat, A. Wagner, and M.E. Cates, New J. Phys. , () submitted
 - [12] J. Eggers, Rev. Mod. Phys. **69**, 865 (1997)
 - [13] I. Cohen, M.P. Brenner, J. Eggers, and S.R. Nagel Phys. Rev. Lett. **83**, 1147 (1999)
 - [14] J.-C. Desplat, I. Pagonabarraga, and P. Bladon, Comp. Phys. Comm. **134**, 273 (2001)
 - [15] W.R. Osborn, E. Orlandini, M.R. Swift, J. Yeomans, and J.R. Banavar Phys. Rev. Lett. **75**, 4031 (1995)
 - [16] A.J. Wagner, and J.M. Yeomans, Phys. Rev. Lett. **80**, 1429 (1998)
 - [17] A.J. Wagner and M.E. Cates, cond-mat/0101140.
 - [18] It is important to note that the initial noise amplitude in the simulation is the same in all the runs, otherwise it is not possible to compare the values of T_{int} , which depend on the initial time needed to form the first domains.

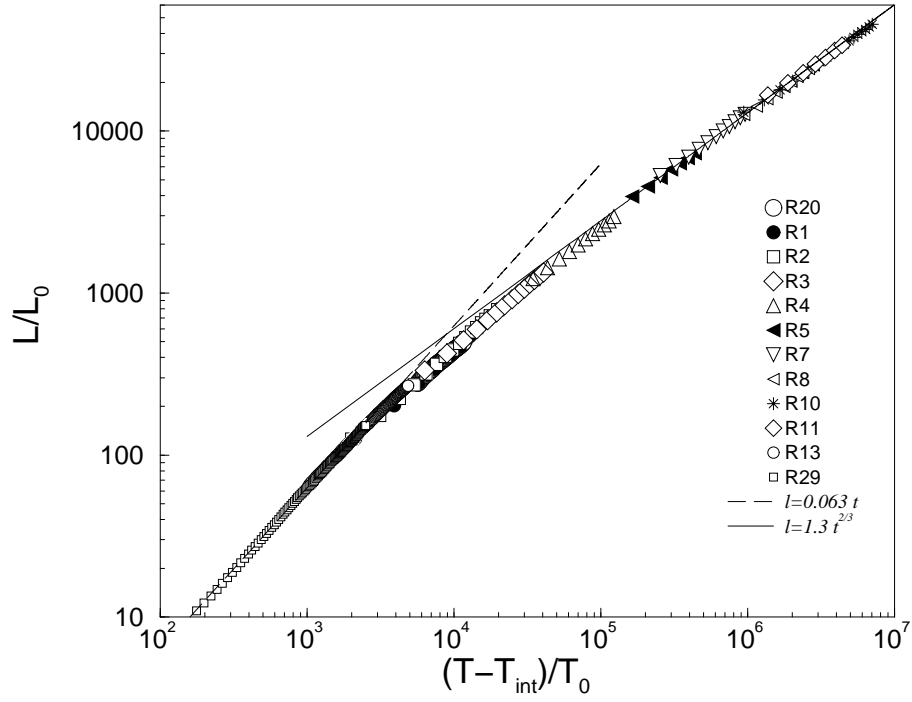


FIG. 1: Scaling plot in reduced variables for the runs of table I. Also shown the asymptotic theoretical predictions with amplitudes fitted from the simulations.

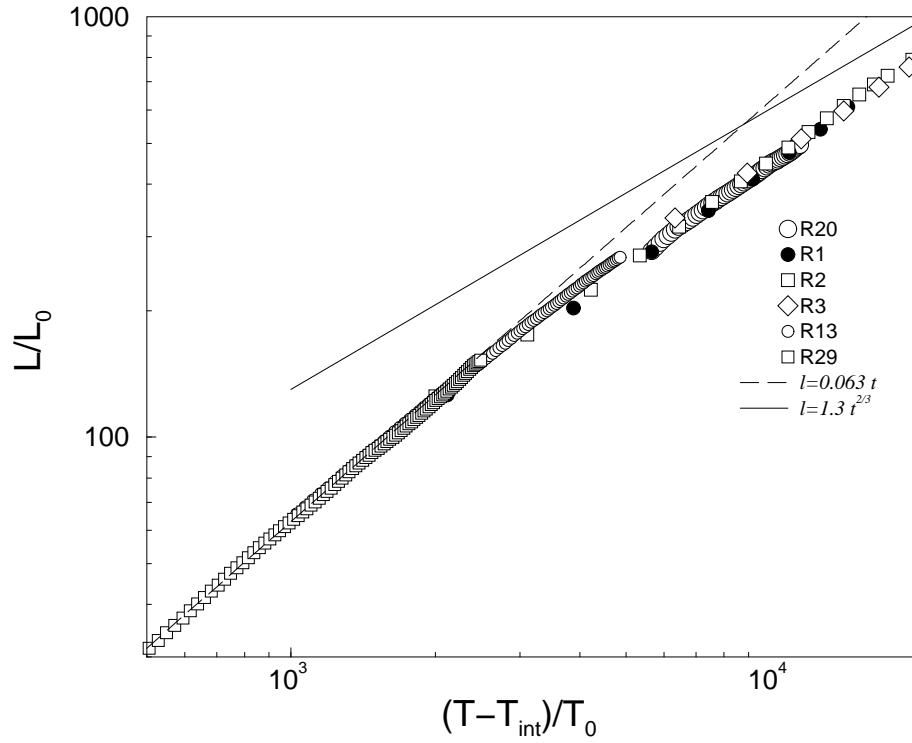


FIG. 2: Scaling plot in reduced variables for the runs of table I that correspond to the transition from the viscous to the crossover regime.

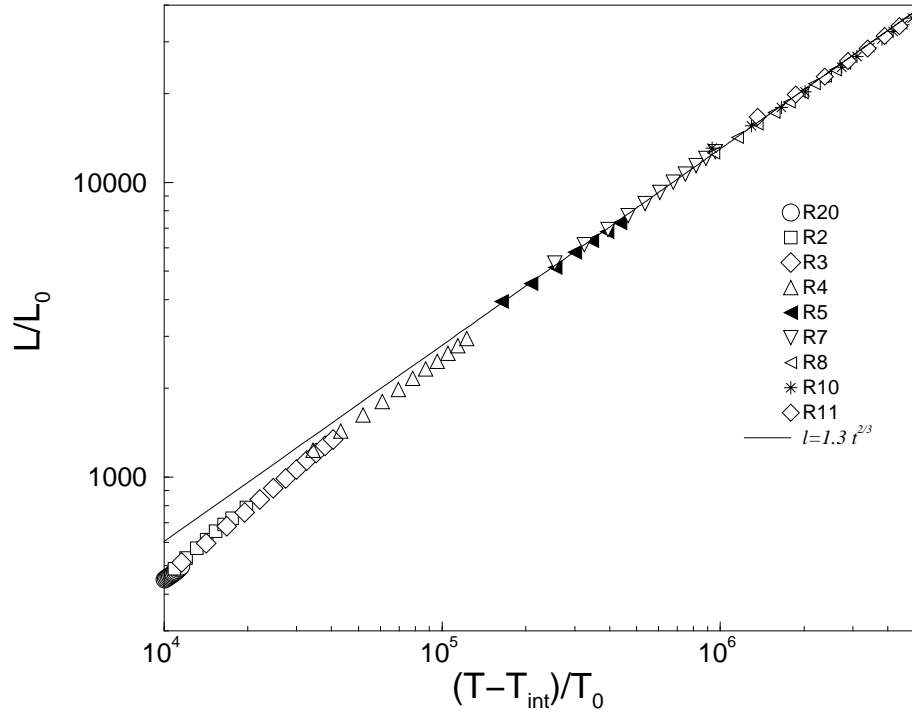


FIG. 3: Scaling plot in reduced variables for the runs of table I that approach the inertial regime.

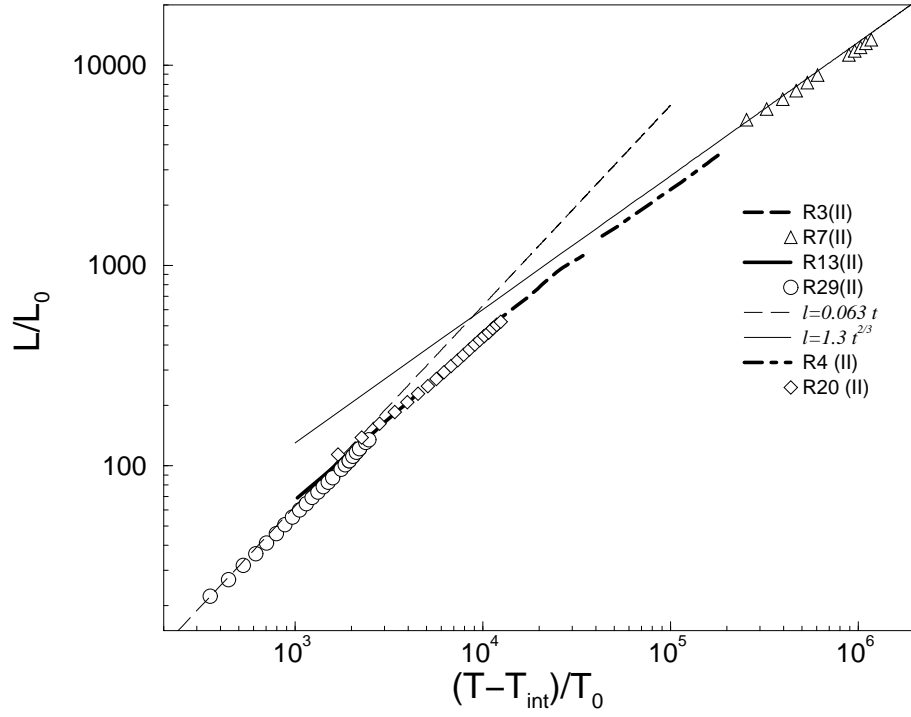


FIG. 4: Scaling plot in reduced variables for the runs of table I computed using eq.(7).

Run number	-A/B	κ	η	M	σ	L_0	t_0
29	0.0625	0.04	0.2	0.3	0.042	0.952	4.54
13	0.00625	0.004	0.035	4.0	0.0042	0.29	2.43
20	0.00625	0.004	0.025	4.0	0.0042	0.15	0.885
1	0.03125	0.02	0.05	1.0	0.021	0.12	0.283
2	0.00625	0.004	0.02	4.0	0.0042	0.095	0.45
3	0.00625	0.004	0.015	4.0	0.0042	0.054	0.19
4	0.00625	0.004	0.01	4.0	0.0042	0.024	0.0567
5	0.0125	0.008	0.0092	2.0	0.0084	0.01	0.011
7	0.00625	0.004	0.005	4.0	0.0042	0.0059	0.00709
8	0.00625	0.004	0.0035	4.0	0.0042	0.0029	0.00243
9	0.00313	0.002	0.00247	8.0	0.0021	0.0029	0.00336
10	0.00313	0.002	0.00183	8.0	0.0021	0.0016	0.00139
11	0.00625	0.004	0.0026	4.0	0.0042	0.0016	0.00099

TABLE I: Parameters of the different runs and characteristic length and times. Run20 corresponds to the notation of Ref.[6].

Run number	29	13	20	1	2	3	4	5	7	8	10	11
T_{int}	1200	700	1000	900	1200	1300	1550	1700	1700	1700	1700	1650

TABLE II: Computed values of the initial time T_{int} .

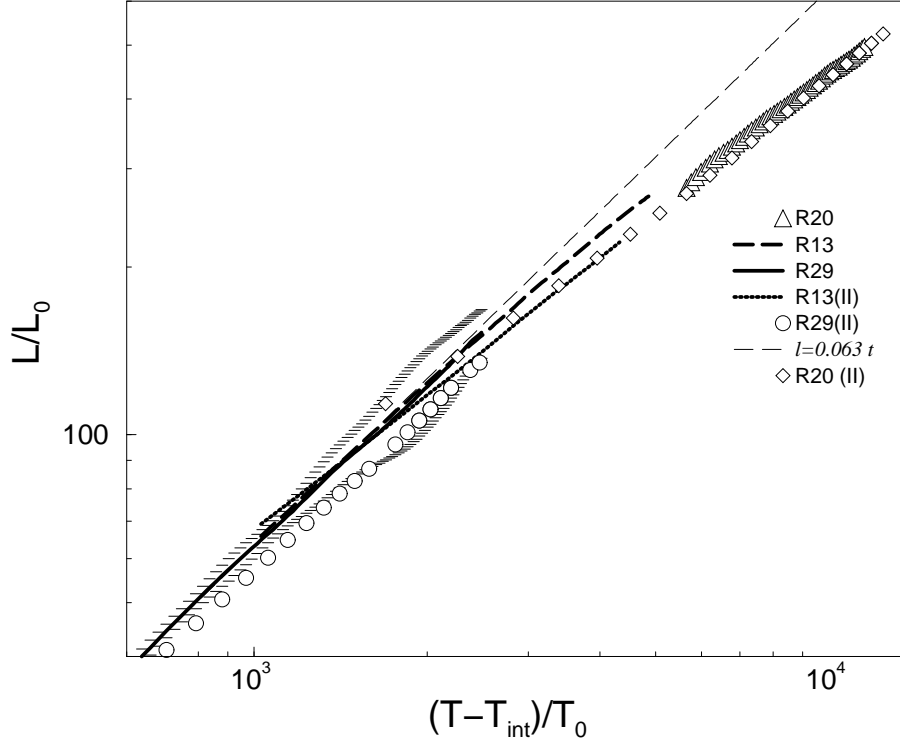


FIG. 5: Comparison of the scaled data computed using eqs.(5) and (7). For run29 we show the estimated error bars in the determination of L from eq.(5) as upper and lower segments.